Original Article

Metallothionein Prevents High-Fat Diet–Induced Cardiac Contractile Dysfunction

Role of Peroxisome Proliferator–Activated Receptor γ Coactivator 1α and Mitochondrial Biogenesis

Feng Dong, Qun Li, Nair Sreejayan, Jennifer M. Nunn, and Jun Ren

Obesity is associated with oxidative stress and mitochondrial and myocardial dysfunction, although interaction among which remains elusive. This study was designed to evaluate the impact of the free radical scavenger metallothionein on high-fat diet–induced myocardial, intracellular Ca^{2+}, and mitochondrial dysfunction. FVB and metallothionein transgenic mice were fed a high- or low-fat diet for 5 months to induce obesity. Echocardiography revealed decreased fractional shortening, increased end-systolic diameter, and cardiac hypertrophy in high-fat–fed FVB mice. Cardiomyocytes from high-fat–fed FVB mice displayed enhanced reactive oxygen species (ROS) production, contractile and intracellular Ca^{2+} defects including depressed peak shortening and maximal velocity of shortening/relengthening, prolonged duration of relengthening, and reduced intracellular Ca^{2+} rise and clearance. Transmission microscopy noted overt mitochondrial damage with reduced mitochondrial density. Western blot analysis revealed enhanced phosphorylation of nuclear factor Foxo3a without changes in Foxo3a, Foxo1a, pFoxo1a, silent information regulator (Sirt), and Akt and pAkt in hearts of high-fat diet–fed FVB mice. The peroxisome proliferator–activated receptor γ coactivator-1α (PGC-1α), a key regulator of mitochondrial biogenesis, was significantly depressed by high-fat diet feeding and in vitro palmitic acid treatment. RT-PCR further depicted reduced levels of the PGC-1α downstream nuclear respiratory factors 1 and 2, mitochondrial transcription factor A, and mitochondrial DNA copy number in hearts of high-fat–fed FVB mice. Intriguingly, the high-fat diet–induced alterations in ROS, myocardial contractile, and mitochondrial and cell signaling were negated by metallothionein, with the exception of pFoxo3a. These data suggest that metallothionein may protect against high-fat diet–induced cardiac dysfunction possibly associated with upregulation of PGC-1α and preservation of mitochondrial biogenesis. *Diabetes* 56:2201–2212, 2007

Clinical and experimental evidence has demonstrated that uncorrected obesity leads to insulin resistance, cardiac hypertrophy, and compromised myocardial contractile function and energy metabolism, which contribute to enhanced cardiovascular morbidity and mortality, as well as risk of developing type 2 diabetes (1–3). Although several scenarios including oxidative stress, dyslipidemia, and hyperleptinemia have been implicated in attributing to obesity-associated cardiac morphological and functional defects (2,4,5), none have been ultimately consolidated, and mechanisms responsible for obesity-associated cardiac dysfunction and aberrant energy metabolism may be tempered by the presence of confounding cardiovascular risk factors such as hypertension and diabetes (6,7). To better understand the mechanism behind obesity-associated cardiac dysfunction, fat-enriched diet is used to foster diet-induced pre-diabetic normotensive or mildly hypertensive obesity (8). Recent evidence from our laboratory as well as others has shown that diet-induced obesity is afflicted with insulin resistance, cardiac hypertrophy, myocardial dysfunction, downregulated mitochondrial oxidative phosphorylation, and biogenesis (8,9). Nonetheless, the pathogenesis of cardiac hypertrophy and contractile dysfunction following high-fat diet intake remains a mystery. Given that oxidative stress is a major risk factor for ventricular hypertrophy and contractile dysfunction (10) and that the levels of intracellular reactive oxygen species (ROS) have been found to be overtly elevated in obesity (2,11), this study was undertaken to examine the impact of the heavy metal scavenger metallothionein on high-fat diet–induced cardiac geometric, morphological, and functional defects. In an effort to elucidate the cellular mechanisms involved in metallothionein and high-fat–induced myocardial alterations, if any, special attention was given to peroxisome proliferator–activated receptor γ coactivator-1α (PGC-1α)-regulated mitochondrial content and function, which are critical in the maintenance of glucose, lipid, and energy metabolism

From the Center for Cardiovascular Research and Alternative Medicine, University of Wyoming, Laramie, Wyoming.

Address correspondence and reprint requests to Dr. Jun Ren, Center for Cardiovascular Research and Alternative Medicine, University of Wyoming, Laramie, WY 82071. E-mail: jren@uwyo.edu.

Received for publication 14 November 2006 and accepted in revised form 10 June 2007.

Published ahead of print at http://diabetes.diabetesjournals.org on 15 June 2007. DOI: 10.2337/db06-1596.

Additional information for this article can be found in an online appendix at http://dx.doi.org/10.2337/db06-1596.

EDD, end-diastolic diameter; ESD, end-systolic diameter; FFI, fura-2 fluorescence intensity; mtDNA, mitochondrial DNA; mtTFA, mitochondrial transcription factor A; NRF, nuclear respiratory factor; PGC-1α, peroxisome proliferator–activated receptor γ coactivator-1α; ROS, reactive oxygen species; Sirt, silent information regulator; TPS, time to peak shortening; TR_{90}, time to 90% relengthening.

in myocardium (12). PGC-1α activates mitochondrial biogenesis and increases oxidative phosphorylation by facilitating transcription, translation, and activation of the transcription factors necessary for mitochondrial DNA (mtDNA) replication (9,13). Considering the recent finding of PGC-1α to retard Forkhead transcriptional factor–associated protein degradation (14), Foxo1a and Foxo3a, as well as their upstream regulator Akt, were also monitored following high-fat diet treatment in wild-type FVB and metallothionein mice.

RESEARCH DESIGN AND METHODS

High-fat diet feeding and intraperitoneal glucose tolerance test. The experimental procedure described here was approved by our institutional animal use and care committee. In brief, 4-month-old male FVB and cardiac-specific metallothionein overexpression transgenic mice weighing ~20 g were randomly assigned to low-fat (10% of total calorie) or high-fat (45% of total calorie) diets (Research Diets, New Brunswick, NJ) for 5 months. The high-fat diet was calorically rich (4.83 vs. 3.91 kcal/g in low-fat diet) due to higher fat composition. However, the two diets possessed similar nutrient composition. Mice were housed individually in a climate-controlled environment with a 12-h light/dark cycle and free access to diets and water. Fur color was used as a marker for metallothionein (dark brown) or FVB (white) mouse identification. After 5 months of feeding, all mice were fasted for 12 h and then given an intraperitoneal injection of glucose (2 g/kg body wt). Blood samples were drawn from the tail immediately before the glucose challenge, as well as 15, 60, and 120 min thereafter. Serum glucose levels were determined using an Accu-Chek III glucose analyzer (15). Systolic and diastolic blood pressure were examined with a semi-automated, amplified tail-cuff device. Blood insulin levels were measured using a mouse insulin enzyme-linked immunosorbent assay kit.

Echocardiographic assessment. Cardiac geometry and function were evaluated in anesthetized (Avertin 2.5%, 10 μl/g body wt i.p.) mice using a two-dimensional guided M-mode echocardiography (Sonos 5500) equipped with a 15–6 MHz linear transducer. Anterior and posterior wall thickness and diastolic and systolic left ventricular dimensions were recorded from M-mode images using the method adopted by the American Society of Echocardiography. Fractional shortening was calculated from end-diastolic diameter (EDD) and end-systolic diameter (ESD) using the following equation: (EDD − ESD)/EDD. Heart rates were averaged over 10 cardiac cycles (16).

Isolation of cardiomyocytes. After ketamine/xylazine sedation, hearts were removed and perfused with Krebs-Henseleit bicarbonate (KHB) buffer containing (in mmol/l): 118 NaCl, 4.7 KCl, 1.2 $MgSO_4$, 1.2 KH_2PO_4, 25 $NaHCO_3$, 10 HEPES, and 11.1 glucose. Hearts were digested with collagenase D for 20 min. Left ventricles were removed and minced before being filtered. Myocyte yield was ~75% and was not affected by high-fat diet or metallothionein. Only rod-shaped myocytes with clear edges were selected for mechanical and intracellular Ca^{2+} study (15).

Cell shortening/relengthening. Mechanical properties of cardiomyocytes were assessed using an IonOptix soft-edge system (IonOptix, Milton, MA). Myocytes were placed in a chamber mounted on the stage of an Olympus IX-70 microscope and superfused (~2 ml/min at 25°C) with a Krebs-Henseleit bicarbonate buffer containing 1 mmol/l $CaCl_2$. Myocytes were field stimulated at 0.5 Hz unless otherwise stated. Cell shortening and relengthening were assessed including peak shortening, indicating peak contractility; time-to-PS (TPS), indicating contraction duration; time-to-90% relengthening (TR_{90}), indicating relaxation duration; and maximal velocities of shortening/relengthening (±dL/dt), indicating maximal pressure development and decline (15).

Intracellular Ca^{2+} transients. A cohort of myocytes was loaded with fura-2/AM (0.5 μmol/l) for 10 min, and fluorescence intensity was recorded with a dual-excitation fluorescence photomultiplier system (Ionoptix). Myocytes were placed onto an Olympus IX-70 inverted microscope and imaged through a Fluor ×40 oil objective. Cells were exposed to light emitted by a 75W lamp and passed through either a 360- or a 380-nm filter, while being stimulated to contract at 0.5 Hz. Fluorescence emissions were detected between 480 and 520 nm, and qualitative change in fura-2 fluorescence intensity (FFI) was inferred from the FFI ratio at the two wavelengths (360/380). Fluorescence decay time (single or bi-exponential decay) was calculated as an indicator of intracellular Ca^{2+} clearing (15).

Analysis of ROS production. Production of cellular ROS was evaluated by analyzing changes in fluorescence intensity resulting from oxidation of the intracellular fluoroprobe DCF [5-(6)-chloromethyl-2′,7′-dichlorodihydrofluorescein diacetate]. In brief, cardiomyocytes were loaded with 10 μmol/l DCF at 37°C for 30 min. The myocytes were rinsed, and the fluorescence intensity was then measured using a fluorescent microplate reader at an excitation wavelength of 480 nm and an emission wavelength of 530 nm. Untreated cells showed no fluorescence and were used to determine background fluorescence (17).

Transmission electron microscopy. Left ventricles were fixed with 2.5% glutaraldehyde/1.2% acrolein in fixative buffer (0.1 mol/l cacodylate, 0.1 mol/l sucrose, pH 7.4) and 1% osmium tetroxide, followed by 1% uranyl acetate, and dehydrated through a graded series of ethanol concentrations before being embedded in LX112 resin (LADD Research Industries, Burlington, VT). Ultra-thin sections (~50 nm) were cut on the ultramicrotome, stained with uranyl acetate followed by lead citrate, and viewed on a Hitachi H-7000 Transmission Electron Microscope equipped with a 4K × 4K cooled charge-coupled device digital camera (18). Quantitative analyses of mitochondrial size and density were carried out at a magnification of ×4,000. An average of six to seven visual fields was evaluated for each mouse heart.

Western blot analysis. The protein was prepared as described (15). A subset of cardiomyocytes from FVB and metallothionein mice was first incubated at 37°C with free fatty acid palmitic acid (1 mmol/l) (see online supplementary methods [available at http://dx.doi.org/10.2337/db06-1596] for palmitic acid preparation) for 24 h before PGC-1α expression was determined. Samples containing equal amount of proteins were separated on 10% SDS-polyacrylamide gels in a minigel apparatus (Mini-PROTEAN II; Bio-Rad) and transferred to nitrocellulose membranes. The membranes were blocked with 5% milk in Tris-buffered saline with Tween and were incubated overnight at 4°C with anti-Akt, anti-pAkt, anti-Foxo1a, anti-pFoxo1a (Thr24), anti–silent information regulator (Sirt), anti-Foxo3a, anti-pFoxo3a (Thr32), PGC-1α (all at 1:1,000), and anti–β-actin (1:5,000). After immunoblotting, the film was scanned and the intensity of immunoblot bands detected with a Bio-Rad calibrated densitometer.

Total RNA extraction, cDNA synthesis, reverse transcription, and real-time PCR. Total RNA was isolated from left ventricles using the TRIzol reagent (Invitrogen), followed by DNase digestion to eliminate genomic DNA contamination. RNAs were quantified with spectrophotometer A260 readings. Synthesis of cDNA was performed at 37°C for 60 min using 1 μg total RNA in a 20-μl system by Superscript III (Invitrogen). Primers were designed using Beacon Designer 5.0 software. The primers used were as follows: mouse nuclear respiratory factor (NRF)1: sense 5′-CCATCACAGACCGTAGTACA GAC-3′, antisense 5′-TCCATCAGCCACAGCAGAG-3′; NRF2: sense 5′-ATAGT TACCATTGACCAGCCTGTG-3′, antisense 5′-GACCATTGTTTCCTGTTCTGTT CC-3′; and fTAM: sense 5′-AGTCCATAGGCACCGTATTG-3′, antisense 5′-TTAGCACGCTCCACATTCC-3′. The primers for housekeeping gene GAPDH (mouse) were: sense 5′-AATGGTGAAGGTCGGTGTGAAC-3′, antisense 5′-CGTGAGTGGAGTCATACTGGAAC-3′. The real-time PCR was performed by using an iCycler iQ real-time PCR detection system (Bio-Rad) with a SYBR Green qPCR SuperMixes kit (Invitrogen). The thermocycling program was 40 cycles of 95°C for 15 s and 55°C for 45 s with an initial cycle of 95°C for 10 min. The melting curve analysis was performed over the range 55–95°C by monitoring SYBR Green fluorescence with increasing temperature (0.5°C increment with a 10-s interval). PCR-specific products were determined as a clear single peak at the melting curves >80°C. Real-time PCR was duplicated for each cDNA sample. Each gene mRNA level was acquired from the value of the threshold cycle (Ct) of the real-time PCR as related to that of GAPDH using the comparative Ct method through the formula 2 ΔCt (ΔCt = GAPDH Ct − gene of interest Ct) (19).

Determination of mtDNA copy number. The relative amount of heart mtDNA copy number was determined using RT-PCR as described (20). Total DNA was extracted using a Qiagen DNeasy tissue kit; 10 ng DNA was used, and mitochondrial nicotinamide adenine dinucleotide dehydrogenase-5 (ND-5) was the target gene. Primers for ND-5 were: forward 5′TGG ATG ATG GTA CGG ACG AA-3′, reverse 5′-TGC GGT TAT AGA GGA TTG CTT GT-3′. Qualitative RT-PCR was performed using a BioRad real-time thermocycler coupled with SYBR Green technology and the following cycling parameters: stage 1, 50°C for 2 min; stage 2, 95°C for 10 min; and stage 3, 40 cycles at 95°C for 15 s and at 55°C for 45 s. Each sample was analyzed in duplicate. Relative mitochondrial copy number to nuclear copy number was assessed by a comparative threshold cycle method, using β-actin as the internal control.

Data analysis. Data are presented as means ± SEM. Statistical comparison was performed by ANOVA, followed by Newman-Keuls post hoc test. Significance was set at $P < 0.05$.

RESULTS

General feature, ROS, and echocardiographic properties of low- and high-fat–fed mice. High-fat feeding significantly increased body but not organ (liver and kidney) weight compared with low-fat–fed mice. Metallothionein did

TABLE 1
Biometric and echocardiographic parameters of mice fed low- or high-fat diet for 5 months

	FVB-LF	FVB-HF	MT-LF	MT-HF
Body weight (g)	26.27 ± 0.58	31.56 ± 0.83*	27.06 ± 0.47	30.07 ± 1.02*
Liver weight (g)	1.40 ± 0.07	1.56 ± 0.08	1.46 ± 0.06	1.53 ± 0.12
Kidney weight (g)	0.34 ± 0.03	0.43 ± 0.02	0.38 ± 0.03	0.43 ± 0.03
Plasma insulin (ng/ml)	0.16 ± 0.01	7.31 ± 0.53*	0.20 ± 0.04	7.01 ± 0.92*
Diastolic blood pressure (mmHg)	72.8 ± 4.8	82.4 ± 4.6	71.8 ± 6.5	81.5 ± 7.9
Systolic blood pressure (mmHg)	101.8 ± 6.9	115.0 ± 5.3	99.6 ± 8.5	112.8 ± 7.4
Heart rate (bpm)	410 ± 7	429 ± 15	439 ± 34	452 ± 13
Wall thickness (mm)	0.84 ± 0.03	0.87 ± 0.04	0.97 ± 0.07	0.87 ± 0.05
EDD (mm)	2.73 ± 0.07	2.81 ± 0.14	2.37 ± 0.17	2.77 ± 0.13
ESD (mm)	1.43 ± 0.09	1.79 ± 0.13*	1.21 ± 0.12	1.43 ± 0.07
LV mass (mg)	69 ± 5	85 ± 7*	72 ± 9	74 ± 5
Normalized LV mass (mg/g)	2.50 ± 0.21	2.62 ± 0.20	2.42 ± 0.24	2.40 ± 0.27
Fraction shortening (%)	48.0 ± 2.6	37.2 ± 1.7*	48.1 ± 3.5	47.7 ± 1.7

Data are means ± SEM. n = 15–16 mice per group. FVB-LF, FVB mice fed a low-fat diet; FVB-HF, mice fed a high-fat diet; MT-LF, metallothionein mice fed a low-fat diet; MT-HF, metallothionein mice fed a high-fat diet. LV, left ventricular. *$P < 0.05$ vs. FVB group.

not affect body or organ weights regardless of the diet regimen. Plasma insulin levels were significantly elevated equally in high-fat diet–fed FVB and metallothionein mice. Blood pressure (both diastolic and systolic), heart rate, wall thickness, left ventricular EDD, and normalized left ventricular mass were comparable among all mouse groups. High-fat feeding significantly increased ESD and left ventricular mass (indication of cardiac hypertrophy) and reduced fractional shortening, which was abrogated by metallothionein transgene. Metallothionein itself did not affect myocardial geometry and fractional shortening (Table 1). Following acute intraperitoneal glucose challenge, serum glucose levels in low-fat–fed FVB or metallothionein mice started to decline after peaking at 15 min and nearly returned to baseline after 120 min. However, postchallenge glucose levels remained at much higher levels between 15 and 120 min in high-fat–fed FVB and metallothionein mice, indicating glucose intolerance. Basal fasting glucose levels were comparable among all groups, excluding the existence of full-blown diabetes. Furthermore, high-fat–fed FVB mouse cardiomyocytes displayed a significantly elevated ROS accumulation, the effect of which was ablated by the metallothionein transgene (Fig. 1).

Cardiomyocyte contractile and intracellular Ca^{2+} properties. Neither high-fat diet nor metallothionein affected resting myocyte length. High-fat feeding significantly reduced peak shortening and ± dL/dt, as well as prolonged TR_{90}, without affecting TPS in cardiomyocytes of FVB mice, somewhat reminiscent of our earlier finding (8). Importantly, metallothionein abolished high-fat diet feeding–induced mechanical abnormalities (Fig. 2). In addition, cardiomyocytes from high-fat–fed mice displayed a significantly elevated baseline intracellular Ca^{2+}, depressed intracellular Ca^{2+} rise in response to electrical stimulus (ΔFFI), and reduced intracellular Ca^{2+} decay rate (either single or bi-exponential curve fit). Metallothionein negated high-fat diet–induced prolongation in intracellular Ca^{2+} decay and depression in ΔFFI with little effect on elevated baseline FFI. Metallothionein itself did not affect any of the intracellular Ca^{2+} properties tested (Fig. 3).

Effect of high-fat diet and metallothionein on stimulus frequency to peak shortening relationship. Mouse hearts beat at high frequencies (>400/min at 37°C). To investigate possible derangement of cardiac excitation-contraction coupling at higher frequencies, the stimulating frequency was increased stepwise from 0.1 to 5 Hz (300

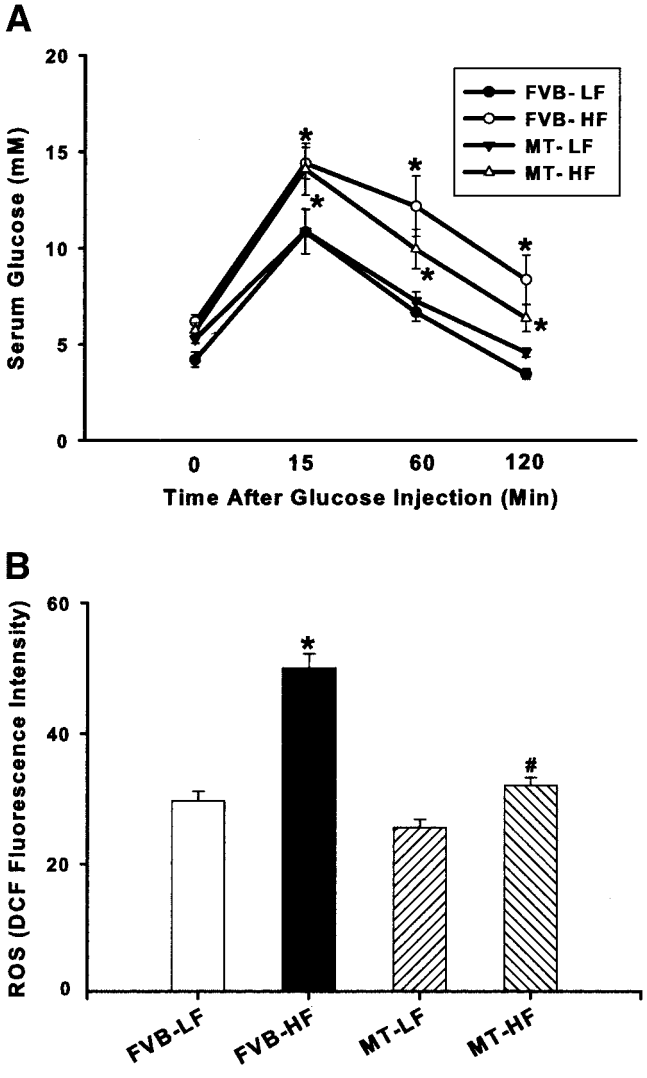

FIG. 1. *A*: Intraperitoneal glucose tolerance test displaying serum glucose concentrations in response to intraperitoneal glucose challenge (2 g glucose/kg body wt). *B*: Cardiomyocyte ROS production in low-fat (LF) and high-fat (HF)–fed FVB and metallothionein (MT) mice. Data are means ± SEM, n = 10–11 mice per group. *$P < 0.05$ vs. FVB-LF group, #$P < 0.05$ vs. FVB-HF group.

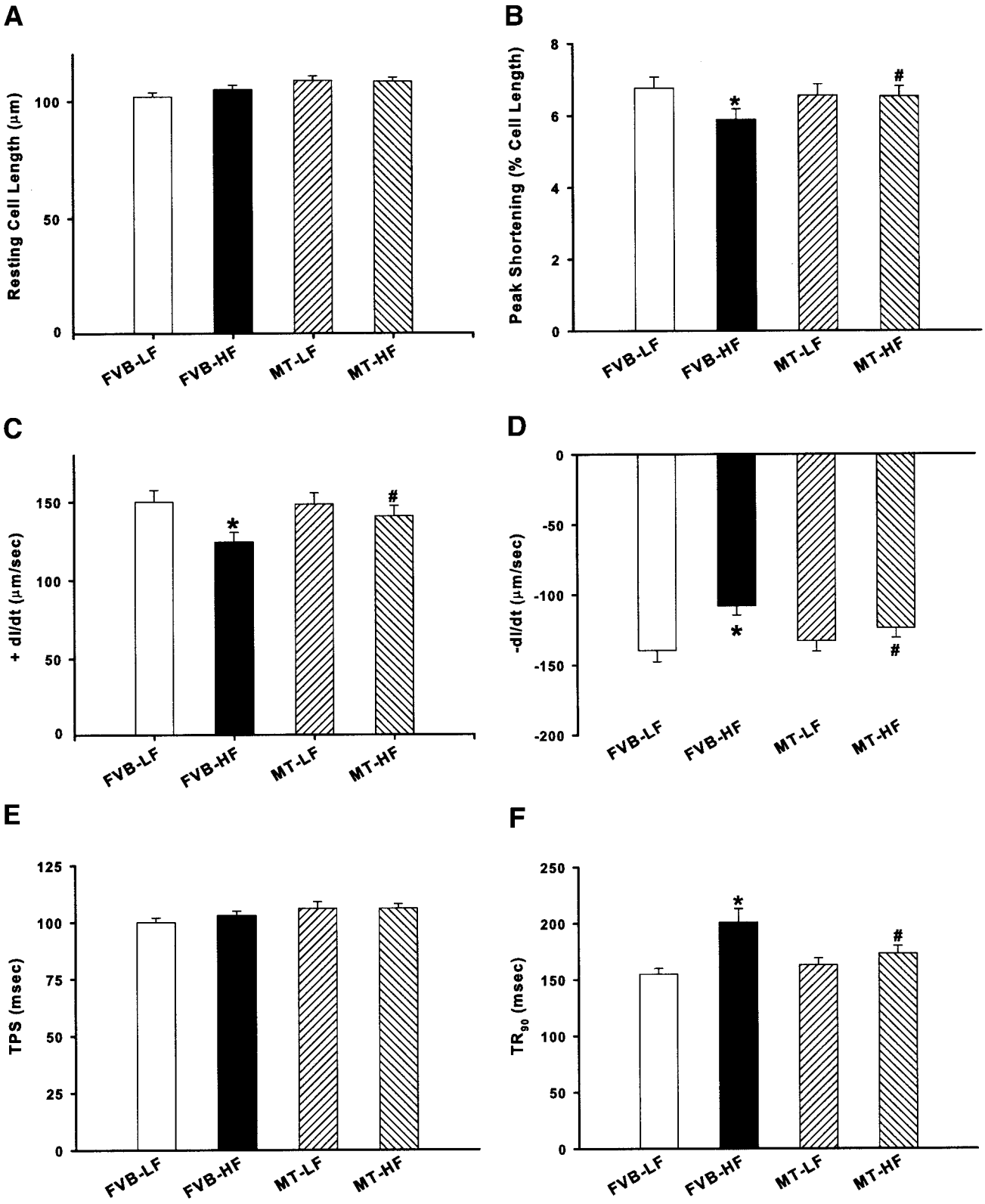

FIG. 2. Contractile properties of cardiomyocytes from low-fat (LF) and high-fat (HF)–fed FVB and metallothionein (MT) mouse hearts. *A*: Resting cell length. *B*: Peak shortening (peak shortening, normalized to cell length). *C*: Maximal velocity of shortening (+ dL/dt). *D*: Maximal velocity of relengthening (−dL/dt). *E*: TPS. *F*: TR_{90}. Data are means ± SEM, n = 133–135 cells/group. *$P < 0.05$ vs. FVB-LF group, #$P < 0.05$ vs. FVB-HF group.

beat/min). Cells were initially stimulated to contract at 0.5 Hz for 5 min to ensure steady state before commencing the frequency protocol. All recordings were normalized to the peak shortening obtained at 0.1 Hz of the same cell. Myocytes from the high-fat–fed group exhibited significantly exaggerated depression in peak shortening at 3.0 and 5.0 Hz without change at low frequencies. Metallothionein transgene itself exerted little effect at all frequencies tested. However, it abrogated high-fat diet–induced depression in peak shortening at 3.0 and 5.0 Hz (Fig. 3*E*).

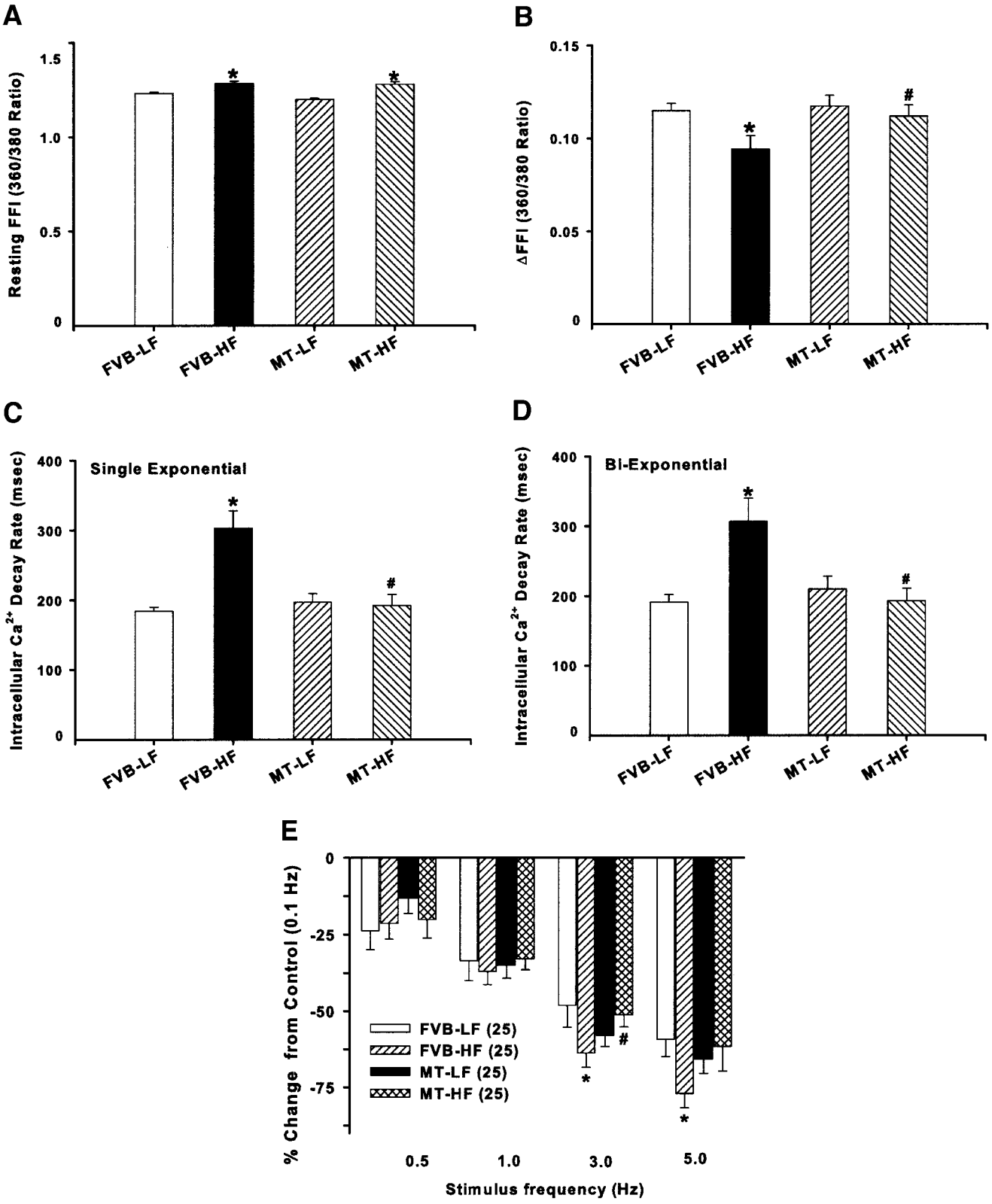

FIG. 3. Intracellular Ca^{2+} transient and stimulus frequency response in cardiomyocytes from low-fat (LF) and high-fat (HF)–fed FVB and metallothionein (MT) mouse hearts. *A*: Resting FFI. *B*: Electrically stimulated rise in FFI (ΔFFI). *C*: Single exponential intracellular Ca^{2+} decay. *D*: Bi-exponential intracellular Ca^{2+} decay. *E*: Peak shortening in response to increased stimulus frequency (0.1–5.0 Hz). Each point represents peak shortening normalized to that of 0.1 Hz of the same cell (cell number provided in parentheses). Data are means ± SEM, n = 68–70 cells/group. *P < 0.05 vs. FVB-LF group, #P < 0.05 vs. FVB-HF group.

Effect of high-fat diet and metallothionein on electron microscopic characteristics of hearts. Without high-fat diet treatment, no ultrastructural difference was noted in cardiac samples between FVB and metallothionein groups (Fig. 4*A* and *B*). High-fat feeding triggered extensive focal damage in hearts of FVB mice character-

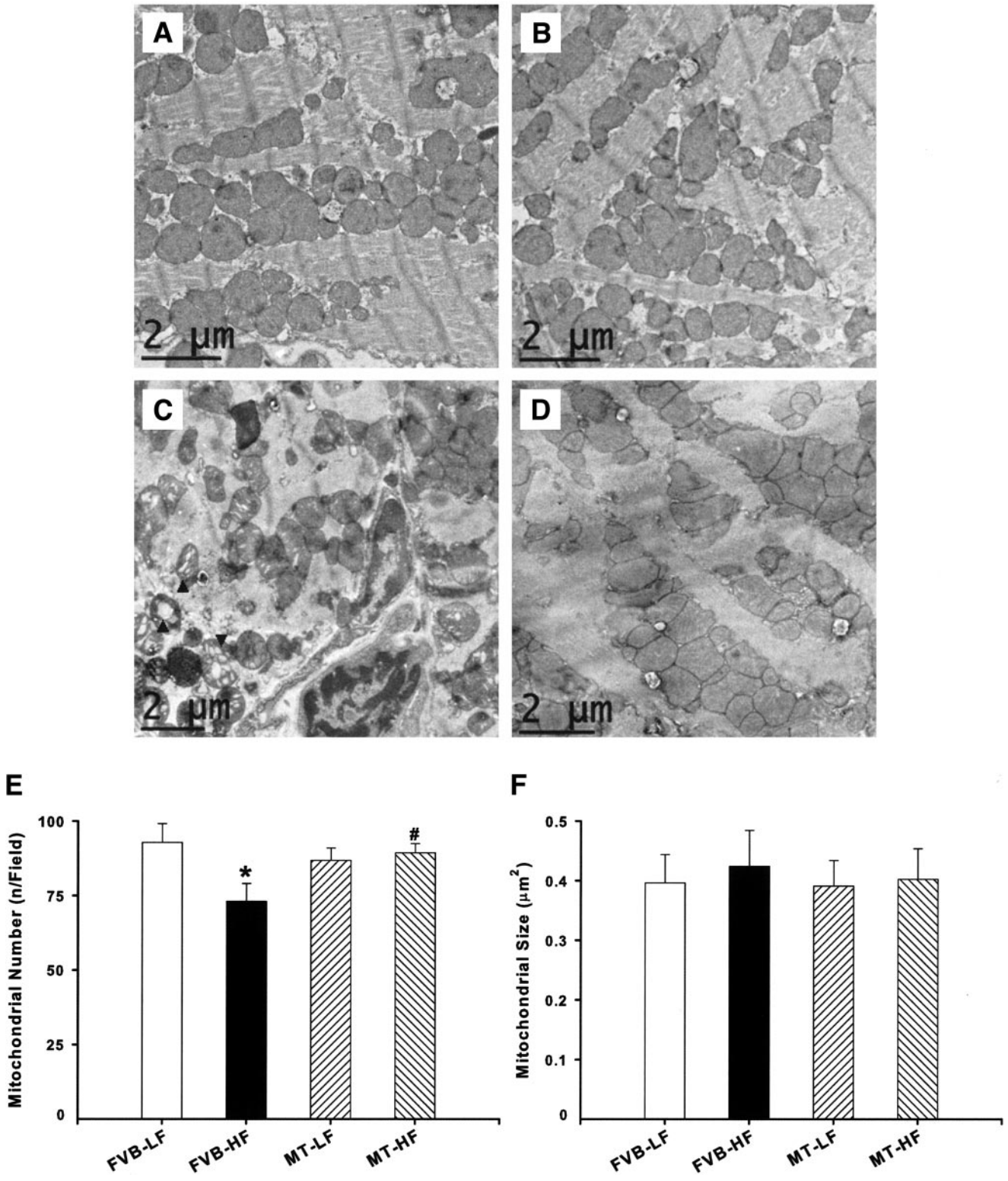

FIG. 4. Transmission electron microscopic micrographs of left ventricular tissues from FVB mice fed a low-fat diet (*A*), metallothionein mice fed a low-fat diet (*B*), FVB mice fed a high-fat diet (*C*), and metallothionein mice fed a high-fat diet (*D*). *A*, *B*, and *D* display regular myofilament and regular mitochondrial structure, whereas *C* displays irregularly shaped mitochondria of cardiomyocytes. ▲, swollen and disorganization of cristae in mitochondria, some with vacuoles, original magnification ×4,000. *E*: Mitochondrial density. *F*: Mitochondrial size. Data are means ± SEM, *n* = 6–7 fields per mouse. **P* < 0.05 vs. FVB-LF group, #*P* < 0.05 vs. FVB-HF group.

ized by mitochondrial swelling, disorganization of cristae, and loss of sarcomere integrity (Fig. 4*C*). Consistent with the mechanical observation, metallothionein negated high-fat diet–induced cardiac structural damage (Fig. 4*D*). Myocardial tissues from high-fat diet–fed metallothionein mice were ultrastructurally indistinguishable from low-fat diet groups. Quantitative analysis revealed that high-fat diet significantly reduced the density but not the size of mitochondria in hearts of FVB mice, the effect of which was nullified by metallothionein (Fig. 4*E* and *F*).

Expression in Akt, pAkt, PGC-1α, Sirt, and PGC-1α downstream factors and mtDNA copy number. To explore the possible mechanism involved in high-fat diet– and metallothionein-induced myocardial morphological and functional responses, the impact of high-fat diet and metallothionein on expression of the cardiac survival factor Akt, the mitochondrial biogenesis regulator PGC-1α, and the caloric-sensitive molecule Sirt was examined. Our results indicated that high-fat diet did not affect expression of Sirt, total and phosphorylated Akt, or pAkt-to-Akt ratio. Metallothionein did not elicit any significant effect on these proteins. Interestingly, high-fat diet significantly downregulated the nuclear receptor coactivator for mitochondrial biogenesis PGC-1α by ~55%. Consistent with its effect on mitochondrial density, metallothionein ablated high-fat diet–induced reduction in PGC-1α (Fig. 5). Further study revealed that high-fat diet– and metallothionein-elicited effects on PGC-1α were mirrored by changes in the PGC-1α downstream factors including NRF1, NRF2, and mitochondrial transcription factor A (mtTFA). While high-fat diet significantly downregulated the levels of NRF1, NRF2, and mtTFA by 70, 40, and 39%, respectively, metallothionein effectively nullified high-fat diet–induced depression of these PGC-1α downstream nuclear factors essential for mitochondrial biogenesis (21) without any effect by itself. The mtDNA copy number, a key index for oxidative mitochondrial damage and mitochondrial biogenesis, was reduced following high-fat diet feeding, the effect of which was reversed by metallothionein (Fig. 6).

Effect of palmitic acid on PGC-1α expression in FVB and metallothionein mouse cardiomyocytes. To examine the causality in metallothionein-elicited protection against high-fat diet–induced downregulation of PGC-1α, we performed an in vitro study to incubate cardiomyocytes with palmitic acid (1 mmol/l) for 24 h. Our immunoblots revealed that palmitic acid significantly downregulated PGC-1α expression in FVB but not in metallothionein mice (Fig. 5*F*), suggesting that free fatty acids may directly downregulate the mitochondrial biogenesis coactivator and play a role in high-fat diet–elicited effects on PGC-1α.

Expression of the Forkhead transcriptional factors Foxo1a and Foxo3a. PGC-1α is known to interact with a number of signaling pathways including the Forkhead transcriptional factors, which may be coactivated by PGC-1α in the regulation of gluconeogenic and heme biosynthetic genes (21). Evaluation in the expression of the Forkhead transcriptional factors Foxo1a and Foxo3a revealed that high-fat diet feeding significantly enhanced Foxo3a phosphorylation without affecting total protein expression of Foxo1a and Foxo3a, as well as the phosphorylation of Foxo1a. Metallothionein failed to alter either the total or phosphorylated form of both Forkhead transcriptional factors under low- or high-fat regimen (Fig. 7).

DISCUSSION

The major findings of our study are that high-fat diet feeding elicits glucose intolerance, cardiac hypertrophy, enhanced ROS accumulation, myocardial contractile dysfunction, impaired intracellular Ca^{2+} handling, mitochondrial damage, and reduced mitochondrial density. The high-fat diet–induced myocardial geometric, functional, and mitochondrial aberrations were associated with depression of mtDNA copy number, the critical mitochondrial activator PGC-1α, as well as its downstream nuclear factors NRF1, NRF2, and mtTFA, indicating a likely role of PGC-1α and its downstream nuclear factors in the reduced mitochondrial biogenesis and myocardial dysfunction under high-fat diet feeding. Intriguingly, the high-fat diet–induced myocardial geometric, functional, and mitochondrial aberrations were significantly attenuated or nullified by metallothionein. Our in vitro study revealed that palmitic acid, a main free fatty acid component in high-fat diet, downregulates PGC-1α expression in cardiomyocytes, the effect of which was ablated by metallothionein. More importantly, high-fat diet–induced depression in mtDNA copy number, PGC-1α, and its downstream nuclear factors NRF1, NRF2, and mtTFA were all restored by metallothionein, consolidating a role of these mitochondrial regulators in high-fat diet–induced cardiac damage and antioxidant-offered cardioprotection. Since metallothionein did not have any "metabolic effect" on glucose metabolism, plasma insulin, or body weight gain, our data suggest that the antioxidant-elicited beneficial effects against high-fat diet–induced myocardial contractile dysfunction and intracellular Ca^{2+} derangement likely result from cardiac-specific effects, including improvement of mitochondrial biogenesis.

High-fat diet intake leads to dyslipidemia, hyperinsulinemia, insulin resistance, obesity, and type 2 diabetes (9,22), all of which trigger cardiac contractile dysfunction via sympathetic activation, renin-angiotensin system stimulation (1,3). Although pharmacological intervention and lifestyle modification including caloric restriction, weight loss, and physical exercise have shown promise in improving the compromised cardiac function in obesity and insulin resistance (3,23), no therapeutic regimen can radically alleviate the devastating heart problems in obese individuals. Our current observation of compromised myocardial and cardiomyocyte contractile function (reduced fraction shortening, enlarged ESD, depressed peak shortening and ± dL/dt, and prolonged TR_{90}) following high-fat diet intake is consistent with previous findings from both human and experimental obesity (3,7,8,24). In addition, these high-fat diet–induced mechanical defects are reminiscent to those reported in full-blown type 1 and type 2 diabetes (2,25,26). However, our 5-month high-fat diet feeding elicited hyperinsulinemia and glucose intolerance with little changes in blood pressure and fasting blood glucose, not favoring contribution of concomitant hypertension and diabetes. The impaired intracellular Ca^{2+} handling shown as elevated resting intracellular Ca^{2+} levels, reduced intracellular Ca^{2+} clearance rate, and reduced intracellular Ca^{2+} rise (ΔFFI) in high-fat diet–fed myocytes of FVB mice is in line with data from a rat model of high-fat diet–induced obesity (8) and is likely responsible for prolonged relaxation, reduced peak shortening, and fraction shortening in hearts of high-fat diet–fed mice. Our observation of exaggerated peak shortening decline at high stimulus frequencies in high-fat–fed mice further supported dampened intracellular Ca^{2+} cycling capacity. The fact that metallothionein reconciled high-fat diet–induced intracellular Ca^{2+} mishandling and intracellular Ca^{2+} cycling suggests an essential role of intracellular Ca^{2+} homeostasis in high-fat diet–induced myocardial dysfunction and antioxidant-offered protection, consistent with our earlier report in a sucrose diet–induced insulin resistance model (15).

Perhaps the most significant finding from our study is that metallothionein restored high-fat diet–induced mitochondrial damage and reduced mitochondrial density,

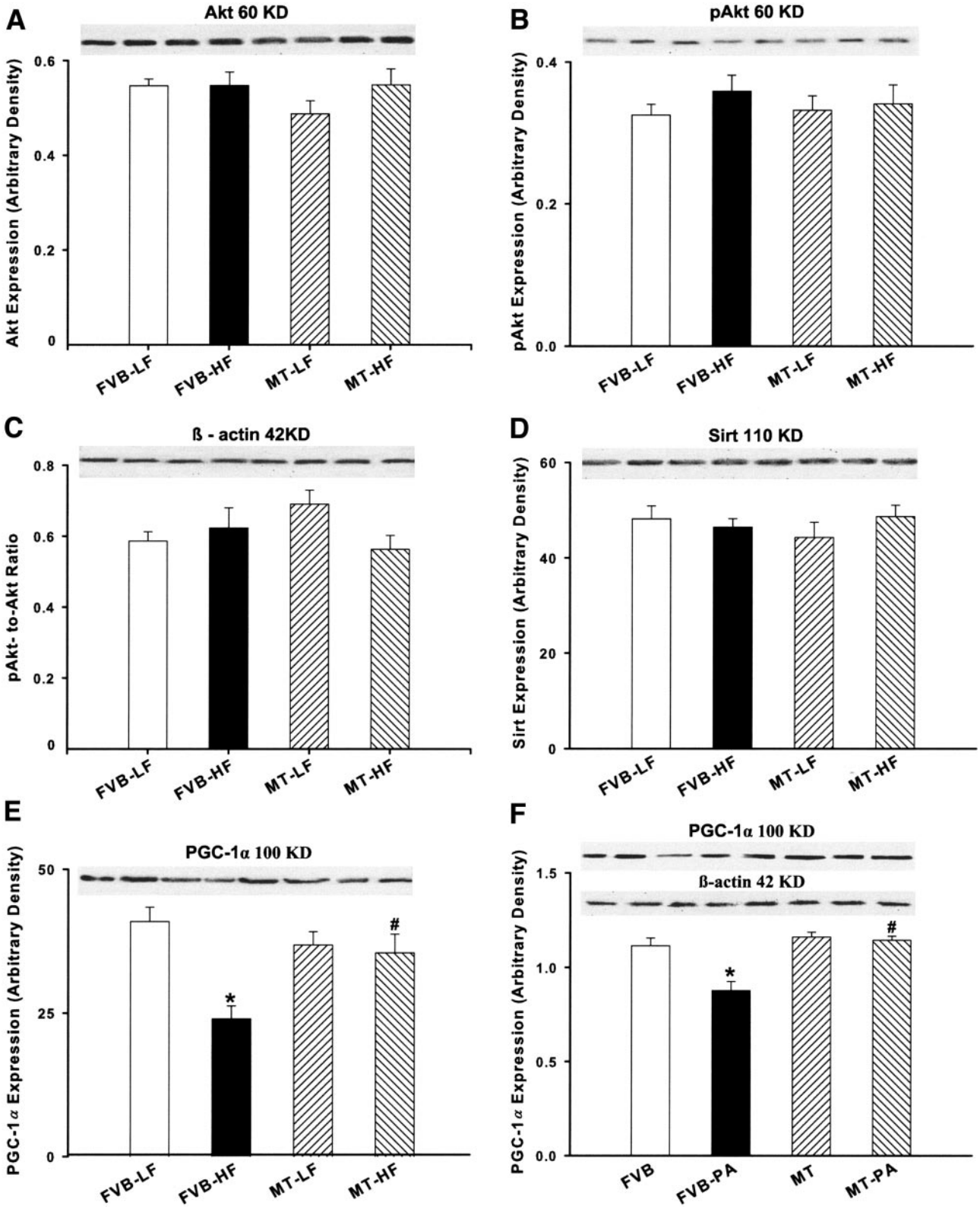

FIG. 5. *A–E*: Western blot analysis of total Akt, pAkt, Sirt, and PGC-1α in myocardium from low-fat (LF) and high-fat (HF)–fed FVB and metallothionein (MT) mice. *A*: Total Akt. *B*: pAkt. *C*: pAkt-to-Akt ratio. *D*: Sirt. *E*: PGC-1α. *F*: PGC-1α expression in FVB and metallothionein (MT) mouse cardiomyocytes incubated with palmitic acid (1 mmol/l) for 24 h. *Insets*: Representative gels of Akt, pAkt, Sirt, PGC-1α, and β-actin (loading control) using specific antibodies (two lanes per group). Data are means ± SEM, n = 8–10 per group. *$P < 0.05$ vs. FVB-LF group, #$P < 0.05$ vs. FVB-HF group.

mtDNA copy number, and downregulation of mitochondrial biogenesis factor PGC-1α and its downstream nuclear factors. Reduced mitochondrial biogenesis and downregulation of genes required for mitochondrial oxidative phosphorylation have been implicated in high-fat diet intake, insulin resistance, and type 2 diabetes (9,27). PGC-1α may induce

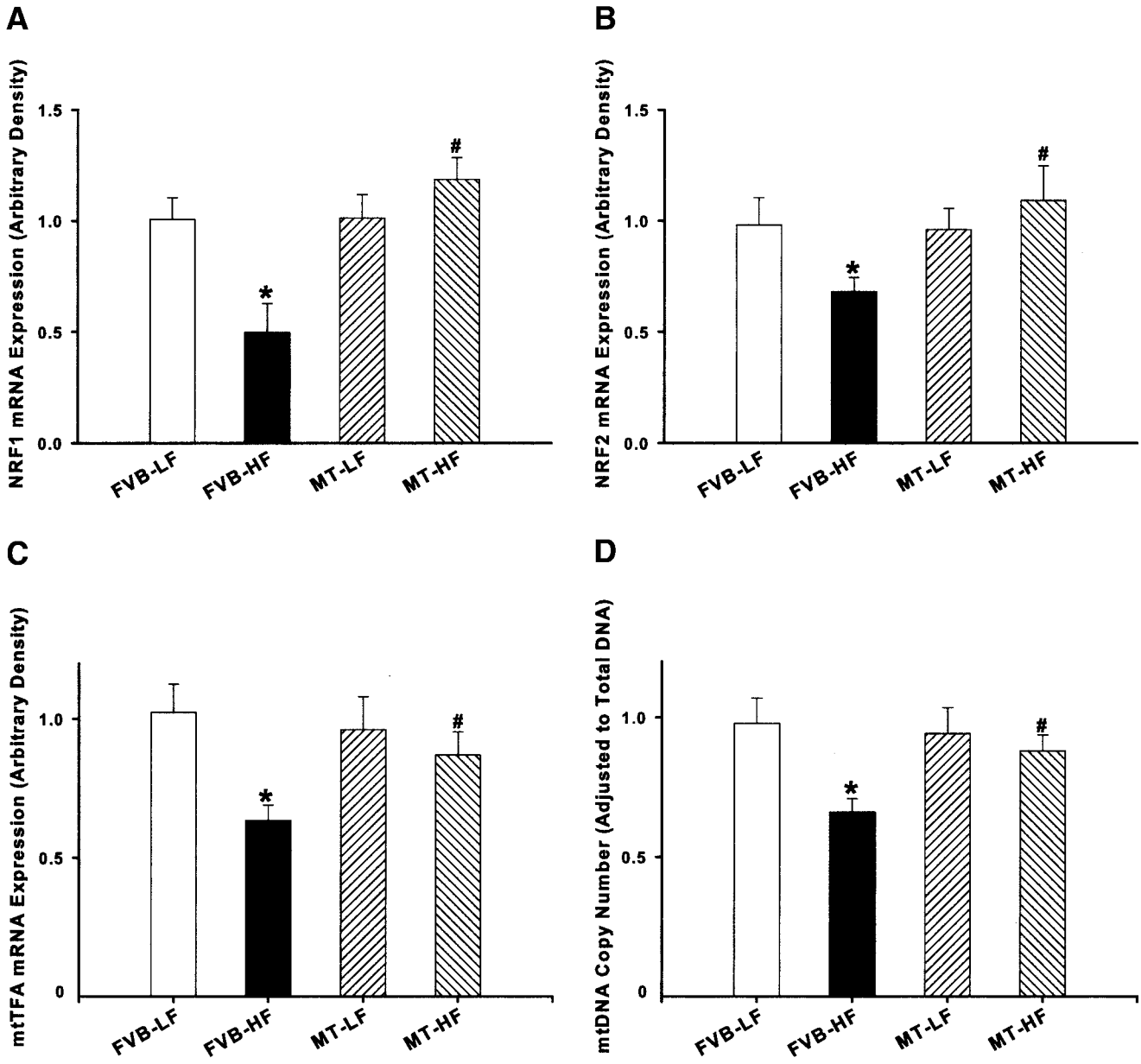

FIG. 6. RT-PCR measurement of NRF1 (*A*), NRF2 (*B*), mtTFA (*C*), and mtDNA copy number (*D*) in left ventricles from low-fat (LF) and high-fat (HF)–fed FVB and metallothionein (MT) mice. Data are means ± SEM, $n = 6–7$. *$P < 0.05$ vs. FVB-LF group, #$P < 0.05$ vs. FVB-HF group.

mitochondrial genes by enhancing levels of NRF1 and NRF2, alternatively called GA-binding protein (GABP), and facilitate GABP binding to regulatory regions of mtTFA promoter (21). It is reasonable to speculate that high-fat diet–induced downregulation of PGC-1α and its downstream nuclear factors (NRF1, NRF2, and mtTFA) may underscore reduced mitochondrial biogenesis and mitochondrial density. This is consolidated by our observation that palmitic acid directly downregulates expression of PGC-1α in cardiomyocytes from FVB but not metallothionein mice. Levels of palmitic acid, the predominant saturated free fatty acids released from adipose tissue, are usually elevated in inflammatory conditions such as obesity, insulin resistance, and diabetes and play an essential role in cardiovascular complications including mitochondrial damage and cardiac dysfunction under these disease states (28). PGC-1α seems to be essential for normal heart function as PGC-1α knockout or deficiency results in diminished cardiac function and heart failure (21,29), suggesting that decreased PGC-1α expression is maladaptive in heart disease. The cellular mechanism responsible for downregulated PGC-1α following high-fat diet intake is not fully clear, although posttranslational modification such as oxidative stress may play a role (21). It was demonstrated that deacetylation of PGC-1α through Sirt increases PGC-1α activity on hepatic gluconeogenic gene transcription (21,30), although our data did not favor any role of Sirt in the regulation of PGC-1α. The observation that antioxidant metallothionein rescues downregulated PGC-1α and its downstream nuclear factors suggests a role of oxidative stress in the regulation of PGC-1α, consistent with our ROS data. Metallothionein has been shown to offer protection against diabetic cardiomyocyte dysfunction through its antioxidant action (26,31). Nonetheless, further study is warranted to define the mechanism responsible for high-fat– and antioxidant-induced regulation on PGC-1α expression.

In our present study, high-fat diet induced Foxo3a

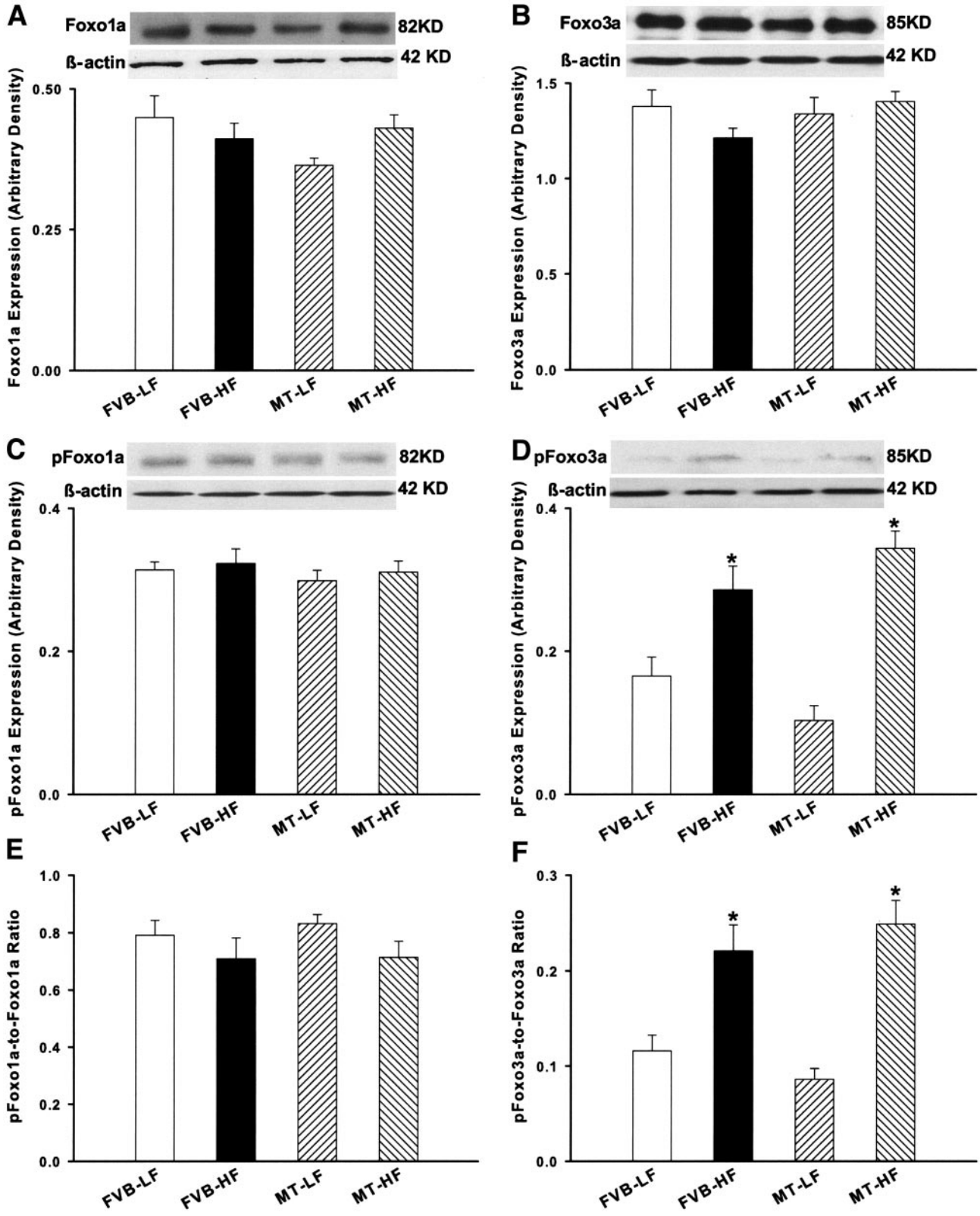

FIG. 7. Western blot analysis exhibiting Foxo1a, Foxo3a, pFoxo1a, and pFoxo3a in ventricles from low-fat (LF) and high-fat (HF)–fed FVB and metallothionein (MT) mice. *A*: Foxo1a. *B*: Foxo3a. *C*: pFoxo1a. *D*: pFoxo3a. *E*: pFoxo1a/Foxo1a. *F*: pFoxo3a/Foxo3a. *Insets*: Representative gel blots of Foxo1a, pFoxo1a, Foxo3a, pFoxo3a, and β-actin using specific antibodies. Data are means ± SEM, $n = 6–8$. *$P < 0.05$ vs. FVB-LF group, #$P < 0.05$ vs. FVB-HF group.

phosphorylation without changes in Akt cascade, Foxo1a phosphorylation, and total Foxo expression. Akt is an essential cardiac survival factor for maintenance of cardiac contractile function (32). Nonetheless, our data did not favor any major role of Akt and its downstream signal Foxo in metallothionein-offered cardioprotection against

high-fat diet intake. Although our observation of enhanced Foxo3a phosphorylation appears to coincide with cardiac hypertrophy under high-fat intake due to inhibition of Forkhead-mediated apoptosis, the fact that metallothionein protects cardiac hypertrophy and myocardial dysfunction against high-fat intake without affecting elevated pFoxo3a levels suggests the contribution of alternate or compensatory mechanisms. In fact, the mitochondrial regulator PGC-1α has been shown recently to suppress Foxo3 transcriptional factor and participate in lysosomal proteolysis and protein degradation (14). However, our study did not identify the interaction between PGC-1α and Forkhead transcription factors.

Concerning experimental limitations, ideally, mice with various pharmacologically or genetically altered metallothionein levels should help to demonstrate whether any robust relationship among high-fat diet feeding, mitochondrial integrity, and myocardial function exists. However, transgenic mice with different metallothionein levels are not readily available, while the pharmacological induction of metallothionein using zinc is rather nonspecific or potentially toxic. Our in vitro incubation of free fatty acid palmitic acid may not truly reflect the metabolic changes elicited by chronic high-fat diet feeding. Due to technical difficulty, we were unable to assess murine cardiomyocyte function following 24 h of palmitic acid treatment, which would provide essential information for high-fat diet–induced myocardial defect. Last but not the least, it was recently reported that resveratrol improves mitochondrial function through decreased PGC-1α acetylation and consequently increased PGC-1α activity (33). However, our results did not favor any role of the protein deacetylase Sirt in high-fat diet– and metallothionein-elicited response, indicating that disparate mechanisms may be present for PGC-1α regulation.

In conclusion, our study offered evidence for the first time that myocardial contractile dysfunction, intracellular Ca^{2+} mishandling, ROS accumulation, mitochondrial damage, and loss of mitochondrial density and mtDNA content in high-fat diet–induced obesity are closely associated with downregulation of mitochondrial biogenesis coactivator PGC-1α and its downstream nuclear factors. In light of metallothionein-elicited protection against high-fat– or palmitic acid–induced cardiac dysfunction, as well as downregulation of the master regulator of mitochondrial biogenesis PGC-1α and its downstream nuclear factors, our data support the novel hypothesis that high-fat diet intake (possibly insulin resistance and type 2 diabetes) impairs mitochondrial biogenesis, which may explain the pathogenesis of aberrant myocardial function under obesity, insulin resistance, and full-blown diabetes. It is imperative that we understand the regulation of PGC-1α and mitochondrial biogenesis under oxidative stress and antioxidant therapy so that treatment strategy may be aimed at achieving sufficient induction of PGC-1α within a therapeutically beneficial window.

ACKNOWLEDGMENTS

This work was supported in part by the American Heart Association Pacific Mountain Affiliate (no. 0355521Z) and the American Diabetes Association (7-0-RA-21) to J.R.

This work was presented in abstract form at the 45th annual meeting of the American Heart Association, Chicago, Illinois, 12–15 November 2006.

The authors thank Dr. D.P. Thomas and C.X. Fang for assistance.

REFERENCES

1. Eckel RH, Barouch WW, Ershow AG: Report of the National Heart, Lung, and Blood Institute-National Institute of Diabetes and Digestive and Kidney Diseases Working Group on the pathophysiology of obesity-associated cardiovascular disease. *Circulation* 105:2923–2928, 2002
2. Li SY, Yang X, Ceylan-Isik AF, Du M, Sreejayan N, Ren J: Cardiac contractile dysfunction in Lep/Lep obesity is accompanied by NADPH oxidase activation, oxidative modification of sarco(endo)plasmic reticulum Ca2+-ATPase and myosin heavy chain isozyme switch. *Diabetologia* 49:1434–1446, 2006
3. Sowers JR: Obesity as a cardiovascular risk factor. *Am J Med* 115 (Suppl. 8A):37S–41S, 2003
4. Nickola MW, Wold LE, Colligan PB, Wang GJ, Samson WK, Ren J: Leptin attenuates cardiac contraction in rat ventricular myocytes: role of NO. *Hypertension* 36:501–505, 2000
5. Zhou YT, Grayburn P, Karim A, Shimabukuro M, Higa M, Baetens D, Orci L, Unger RH: Lipotoxic heart disease in obese rats: implications for human obesity. *Proc Natl Acad Sci U S A* 97:1784–1789, 2000
6. Dobrian AD, Davies MJ, Prewitt RL, Lauterio TJ: Development of hypertension in a rat model of diet-induced obesity. *Hypertension* 35:1009–1015, 2000
7. Dobrian AD, Davies MJ, Schriver SD, Lauterio TJ, Prewitt RL: Oxidative stress in a rat model of obesity-induced hypertension. *Hypertension* 37:554–560, 2001
8. Relling DP, Esberg LB, Fang CX, Johnson WT, Murphy EJ, Carlson EC, Saari JT, Ren J: High-fat diet-induced juvenile obesity leads to cardiomyocyte dysfunction and upregulation of Foxo3a transcription factor independent of lipotoxicity and apoptosis. *J Hypertens* 24:549–561, 2006
9. Sparks LM, Xie H, Koza RA, Mynatt R, Hulver MW, Bray GA, Smith SR: A high-fat diet coordinately downregulates genes required for mitochondrial oxidative phosphorylation in skeletal muscle. *Diabetes* 54:1926–1933, 2005
10. Byrne JA, Grieve DJ, Cave AC, Shah AM: Oxidative stress and heart failure. *Arch Mal Coeur Vaiss* 96:214–221, 2003
11. Keaney JF Jr, Larson MG, Vasan RS, Wilson PW, Lipinska I, Corey D, Massaro JM, Sutherland P, Vita JA, Benjamin EJ: Obesity and systemic oxidative stress: clinical correlates of oxidative stress in the Framingham Study. *Arterioscler Thromb Vasc Biol* 23:434–439, 2003
12. Rolo AP, Palmeira CM: Diabetes and mitochondrial function: role of hyperglycemia and oxidative stress. *Toxicol Appl Pharmacol* 212:167–178, 2006
13. Scarpulla RC: Nuclear activators and coactivators in mammalian mitochondrial biogenesis. *Biochim Biophys Acta* 1576:1–14, 2002
14. Sandri M, Lin J, Handschin C, Yang W, Arany ZP, Lecker SH, Goldberg AL, Spiegelman BM: PGC-1{alpha} protects skeletal muscle from atrophy by suppressing FoxO3 action and atrophy-specific gene transcription. *Proc Natl Acad Sci U S A* 103:16260–16265, 2006
15. Fang CX, Dong F, Ren BH, Epstein PN, Ren J: Metallothionein alleviates cardiac contractile dysfunction induced by insulin resistance: role of Akt phosphorylation, PTB1B, PPARgamma and c-Jun. *Diabetologia* 48:2412–2421, 2005
16. Gardin JM, Siri FM, Kitsis RN, Edwards JG, Leinwand LA: Echocardiographic assessment of left ventricular mass and systolic function in mice. *Circ Res* 76:907–914, 1995
17. Privratsky JR, Wold LE, Sowers JR, Quinn MT, Ren J: AT1 blockade prevents glucose-induced cardiac dysfunction in ventricular myocytes: role of the AT1 receptor and NADPH oxidase. *Hypertension* 42:206–212, 2003
18. Dong F, Zhang X, Yang X, Esberg LB, Yang H, Zhang Z, Culver B, Ren J: Impaired cardiac contractile function in ventricular myocytes from leptin-deficient ob/ob obese mice. *J Endocrinol* 188:25–36, 2006
19. Kinkel MD, Horton WE Jr: Coordinate down-regulation of cartilage matrix gene expression in Bcl-2 deficient chondrocytes is associated with decreased SOX9 expression and decreased mRNA stability. *J Cell Biochem* 88:941–953, 2003
20. Stites T, Storms D, Bauerly K, Mah J, Harris C, Fascetti A, Rogers Q, Tchaparian E, Satre M, Rucker RB: Pyrroloquinoline quinone modulates mitochondrial quantity and function in mice. *J Nutr* 136:390–396, 2006
21. Handschin C, Spiegelman BM: Peroxisome proliferator-activated receptor gamma coactivator 1 coactivators, energy homeostasis, and metabolism. *Endocr Rev* 27:728–735, 2006
22. Axen KV, Dikeakos A, Sclafani A: High dietary fat promotes syndrome X in nonobese rats. *J Nutr* 133:2244–2249, 2003
23. Matthaei S, Stumvoll M, Kellerer M, Haring HU: Pathophysiology and

pharmacological treatment of insulin resistance. *Endocr Rev* 21:585–618, 2000
24. de Divitiis O, Fazio S, Petitto M, Maddalena G, Contaldo F, Mancini M: Obesity and cardiac function. *Circulation* 64:477–482, 1981
25. Norby FL, Aberle NS, Kajstura J, Anversa P, Ren J: Transgenic overexpression of insulin-like growth factor I prevents streptozotocin-induced cardiac contractile dysfunction and beta-adrenergic response in ventricular myocytes. *J Endocrinol* 180:175–182, 2004
26. Ye G, Metreveli NS, Ren J, Epstein PN: Metallothionein prevents diabetes-induced deficits in cardiomyocytes by inhibiting reactive oxygen species production. *Diabetes* 52:777–783, 2003
27. Boirie Y: Insulin regulation of mitochondrial proteins and oxidative phosphorylation in human muscle. *Trends Endocrinol Metab* 14:393–394, 2003
28. Wilson-Fritch L, Nicoloro S, Chouinard M, Lazar MA, Chui PC, Leszyk J, Straubhaar J, Czech MP, Corvera S: Mitochondrial remodeling in adipose tissue associated with obesity and treatment with rosiglitazone. *J Clin Invest* 114:1281–1289, 2004
29. Arany Z, Novikov M, Chin S, Ma Y, Rosenzweig A, Spiegelman BM: Transverse aortic constriction leads to accelerated heart failure in mice lacking PPAR-gamma coactivator 1alpha. *Proc Natl Acad Sci U S A* 103:10086–10091, 2006
30. Rodgers JT, Lerin C, Haas W, Gygi SP, Spiegelman BM, Puigserver P: Nutrient control of glucose homeostasis through a complex of PGC-1alpha and SIRT1. *Nature* 434:113–118, 2005
31. Wold LE, Ceylan-Isik AF, Fang CX, Yang X, Li SY, Sreejayan N, Privratsky JR, Ren J: Metallothionein alleviates cardiac dysfunction in streptozotocin-induced diabetes: role of Ca2+ cycling proteins, NADPH oxidase, poly-(ADP-Ribose) polymerase and myosin heavy chain isozyme. *Free Radic Biol Med* 40:1419–1429, 2006
32. Latronico MV, Costinean S, Lavitrano ML, Peschle C, Condorelli G: Regulation of cell size and contractile function by AKT in cardiomyocytes. *Ann N Y Acad Sci* 1015:250–260, 2004
33. Lagouge M, Argmann C, Gerhart-Hines Z, Meziane H, Lerin C, Daussin F, Messadeq N, Milne J, Lambert P, Elliott P, Geny B, Laakso M, Puigserver P, Auwerx J: Resveratrol improves mitochondrial function and protects against metabolic disease by activating SIRT1 and PGC-1alpha. *Cell* 127:1109–1122, 2006